

Perception of Time-Discrete Haptic Feedback on the Waist Is Invariant With Gait Events

I. Cesini¹, E. Martini¹, M. Filosa, G. Spigler, A. M. Sabatini, N. Vitiello², C. M. Oddo², and S. Crea¹

Abstract—The effectiveness of haptic feedback devices highly depends on the perception of tactile stimuli, which differs across body parts and can be affected by movement. In this study, a novel wearable sensory feedback apparatus made of a pair of pressure-sensitive insoles and a belt equipped with vibrotactile units is presented; the device provides time-discrete vibrations around the waist, synchronized with biomechanically-relevant gait events during walking. Experiments with fifteen healthy volunteers were carried out to investigate users' tactile perception on the waist. Stimuli of different intensities were provided at twelve locations, each time synchronously with one pre-defined gait event (i.e. heel strike, flat foot or toe off), following a pseudo-random stimulation sequence. Reaction time, detection rate and localization accuracy were analyzed as functions of the stimulation level and site and the effect of gait events on perception was investigated. Results revealed that above-threshold stimuli (i.e. vibrations characterized by acceleration amplitudes of 1.92g and 2.13g and frequencies of 100 Hz and 150 Hz, respectively) can be effectively perceived in all the sites and successfully localized when the intertactor spacing is set to 10 cm. Moreover, it was found that perception of time-discrete vibrations was not affected by phase-related gating mechanisms, suggesting that the waist could be considered as a preferred body region for delivering haptic feedback during walking.

Index Terms—Gait events, haptic display, mobile applications, perception, reaction time, sensory augmentation, sensory feedback, vibrotactile stimulation, waist, wearable haptics.

I. INTRODUCTION

HAPTIC feedback has been widely proposed to augment or restore missing sensory information. The development of effective sensory feedback devices highly depends on the perception of the provided stimuli, which, for sake of wearability issues, can be delivered on low-sensitive body areas. Spatial and temporal acuity of tactile stimuli vary significantly across human body parts, being greatest at the

Manuscript received May 31, 2019; revised February 28, 2020; accepted March 29, 2020. Date of publication April 24, 2020; date of current version July 8, 2020. This work was supported in part by the EU within the CYBERLEGS Plus Plus project (H2020-ICT-2016-1) under Grant 731931 and in part by the Italian National Institute for Insurance against Accidents at Work (INAIL Centro Protesi, Budrio) within the MOTU project. (Corresponding authors: I. Cesini; S. Crea.)

I. Cesini, E. Martini, M. Filosa, A. M. Sabatini, and C. M. Oddo are with The BioRobotics Institute, Scuola Superiore Sant'Anna, 56127 Pisa, Italy (e-mail: i.cesini@santannapisa.it).

G. Spigler is with the Tilburg School of Humanities and Digital Sciences, Department of Cognitive Science and Artificial Intelligence, 5037 AB Tilburg, The Netherlands.

N. Vitiello and S. Crea are with The BioRobotics Institute, Scuola Superiore Sant'Anna, 56127 Pisa, Italy, and also with IRCSS Fondazione Don Carlo Gnocchi, 20162 Milan, Italy (e-mail: simona.crea@santannapisa.it).

Digital Object Identifier 10.1109/TNSRE.2020.2984913

fingers and dropping at sites close to the abdomen [1]. The spatial and temporal resolving power of the skin and the influence of factors such as body locus are relevant for tactile rendering via haptic displays. In recent years, haptic wearable devices have been widely explored for sensory augmentation in a variety of application domains, including spatial orientation [2]–[6], virtual reality [7], telepresence [8] and sensory substitution [9]–[12]. Especially in dynamic contexts, in which augmented sensory information is used for navigation aid or as cue for gait events during locomotion, the execution of motor tasks can alter the cutaneous perception, resulting in the loss of crucial information and limiting the effectiveness of the feedback system.

A very common approach to provide haptic feedback is by means of vibrotactile (VT) stimulation, whose intensity and frequency can be modulated to convey different types of information. In this scenario, identifying VT intensity and frequency perception thresholds at different body sites is paramount to deliver effective stimulation. With the goal to develop VT-based lower-limb sensory feedback devices, few studies investigated VT perception on different body areas, most of which were carried out in static, very-structured, experimental conditions [13]–[16]. However, one of the most critical factors influencing tactile perception during dynamic voluntary movements such as walking is the underlying muscle activation. Many neurophysiological studies evidenced that perception is attenuated when the stimulated area is actively involved in the movement [17]–[21] and gait phases affect the perceived intensity of cutaneous input [22]. Furthermore, stimulating specific nerves during the step cycle may lead to different sensation gating mechanisms [15]. Such perception modulation was confirmed by Jiang and Hannaford [23] who demonstrated that lower-limb sites (i.e. toes and thighs) during walking exhibit higher reaction times to VT stimuli with respect to static conditions or to the upper body sites (i.e. waist and wrists). Similar experiments were carried out by Karuei *et al.* [24] who reported that walking significantly reduced detection performance even with high intensity vibrations, and the perception on thigh and feet were the most affected by movement. In their study, Husman *et al.* [25] analyzed the perceptibility of skin stretch stimuli of different intensities applied to the thigh during static and walking conditions, finding that high magnitude stimuli were accurately perceived in both conditions and low intensity stimuli remained almost unnoticed during walking. In general, all these studies agree in reporting a strong movement-induced attenuation of perception when stimuli were applied to lower limbs, however a systematic analysis of the influence of gait phases was never

performed. In particular, limbs muscle activity and the high reaction forces produced by certain gait events, e.g. heel-strike, might mask lower intensity stimuli and result in a non-uniform perception throughout the gait cycle. In the light of the findings reported above, lower limbs may not be a preferable choice as stimulation site for haptic feedback in mobile contexts.

A possible alternative to lower limbs for delivering haptic feedback in dynamic conditions is the waist. Although it presents higher perception threshold and lower spatial acuity than other loci [26], [27], the abdomen offers an extensive area for presenting tactile information [28] and the underlying muscles present relatively-low activations during locomotion. Furthermore, through the torso, spatial information can be conveyed in an intuitive way since the stimuli are directly mapped to the body coordinates. In the field of gait rehabilitation, few research groups applied VT stimuli to the torso for improving postural control [29]–[32] or providing foot-ground contact information [33], [34], while the main targeted site for haptic feedback remained the thigh [10], [13], [15], [35]–[39]. On the other hand, most of the studies on haptic displays for visually impaired persons focused on the delivery of VT stimuli on the abdomen to indicate a direction of travel [2], [4]–[6], [28]. In these applications, it is essential for the user to promptly perceive and accurately localize the stimuli.

A comprehensive study on tactile perception and stimuli localization accuracy across the torso was performed by Cholewiak *et al.* [40] who analyzed human's ability to detect and localize vibratory stimuli at different loci around the abdomen. The authors found that detection thresholds did not change across stimulation sites, while remarkable differences were found over the sites tested in terms of localization accuracy, with higher performance encountered near the navel and the spine. Similarly, Van Erp and colleagues performed several studies [3], [4], [41], [42] in attempt to understand the spatial characteristics of VT perception on the torso, finding that sensitivity for tactile stimuli was greater on the abdomen than on the back, and it decreased the further the stimulus point was from the sagittal plane. The experiments hereby reported provide a useful characterization on the abdomen as a stimulation site for haptic interfaces, however they were all performed in static conditions, and to the best of the authors' knowledge, there are no studies reported in literature investigating how tactile perception across different loci on the torso is influenced by the action of walking.

In this study, human's ability to perceive and localize time-discrete VT stimuli applied on the abdomen was investigated during walking. Stimuli were delivered at twelve locations around the waist, at the occurrence of specific gait events, using a set of vibrating motors integrated in a belt [33]. Detection and localization accuracy of vibrations were investigated over the stimulation sites tested and the influence of specific gait events on perception was analyzed.

II. MATERIALS AND METHODS

Participants walked on the treadmill wearing the sensory feedback device and holding a button (Fig. 1a). The wearable sensory feedback apparatus is made of a pair of pressure-sensitive insoles and a belt equipped with twelve VT units

equally spaced 5 cm apart around the abdominal circumference. The device is a revised version of the one presented in [10], [15], which was designed to provide unilateral VT stimulations at the thigh or waist areas to lower-limb amputees. During the experiments the VT units were activated at the occurrence of specific gait events (i.e. heel strike, flat foot and toe off) at three different activation levels, namely $\delta_{1.48g}$, $\delta_{1.92g}$, and $\delta_{2.13g}$ (Fig. 1b). When the subject perceived a stimulus, s/he pressed the button and specified the stimulation site. For locating the stimuli, the subject relied on a map displaying VT units positions on the waist (Fig. 1a). In this section, along with the description of the sensory feedback device, also called bidirectional interface (BI), details about the experimental setup and protocol are provided.

A. Wearable Vibrotactile Bidirectional Interface

The BI is composed of three modules: (i) a *sensing* module, consisting of a pair of pressure-sensitive insoles for real-time measurement of the vertical ground reaction force; (ii) a *mapping* module, encoding gait information into discrete stimuli, according to a discrete-event based sensory feedback control (DESC) approach [12]; (iii) a *feedback* module, i.e. a set of VT transducers attached to a textile belt (Fig. 1a).

Each pressure-sensitive insole includes 16 optoelectronic sensors, based on the technology described in [43], [44]. Sensor signals are acquired through onboard electronics placed on the shoe dorsum, integrating a microcontroller (STM32L476RG, STMicroelectronics) and a 16-channels multiplexer (ADG 1606, Analog Devices) for analog-to-digital conversion. An Ultra-Wide Band (UWB) transceiver module (DWM1000, DecaWave, 6.8 Mbps data rate) wirelessly sends sensors data to the mapping module. Compared to other wireless communication solutions (e.g. Bluetooth) UWB allows transmission of large amounts of data at high rates and with low package losses [45].

The mapping module consists of two custom electronic boards: the so-called *Mezzanine* board is used for wireless acquisition of insole signals and communicates with the *VibroBoard* through a standard SPI bus. The board integrates a UWB transceiver (DWM1000, DecaWave, 6.8 Mbps data rate) and a dedicated microprocessor (STM32 ST Microelectronics). The *VibroBoard* houses a NI System On Module SbRIO-9651 (National InstrumentsTM) including a Real Time processor and FPGA (Xilinx Zynq-7000, 667 MHz). The FPGA manages SPI communication with the *Mezzanine* and drives the vibrating motors, while the Real Time processor implements the high-level algorithms (100Hz) for gait-phase segmentation based on the sampled insole data and activation of the vibrating units. A graphical user interface (GUI) runs on a computer, connected via UDP to run the system, visualize data in real time and set the stimulation parameters. The *VibroBoard* further integrates a power-management stage and a set of twelve motor drivers. A lithium polymer battery (Li-ION 11.1V) guarantees a system autonomy of 3 hours. The electronics is enclosed in a 3D printed box, attached to the belt of the feedback module (Fig. 1a), resulting in an overall weight of the belt of about 500 g.

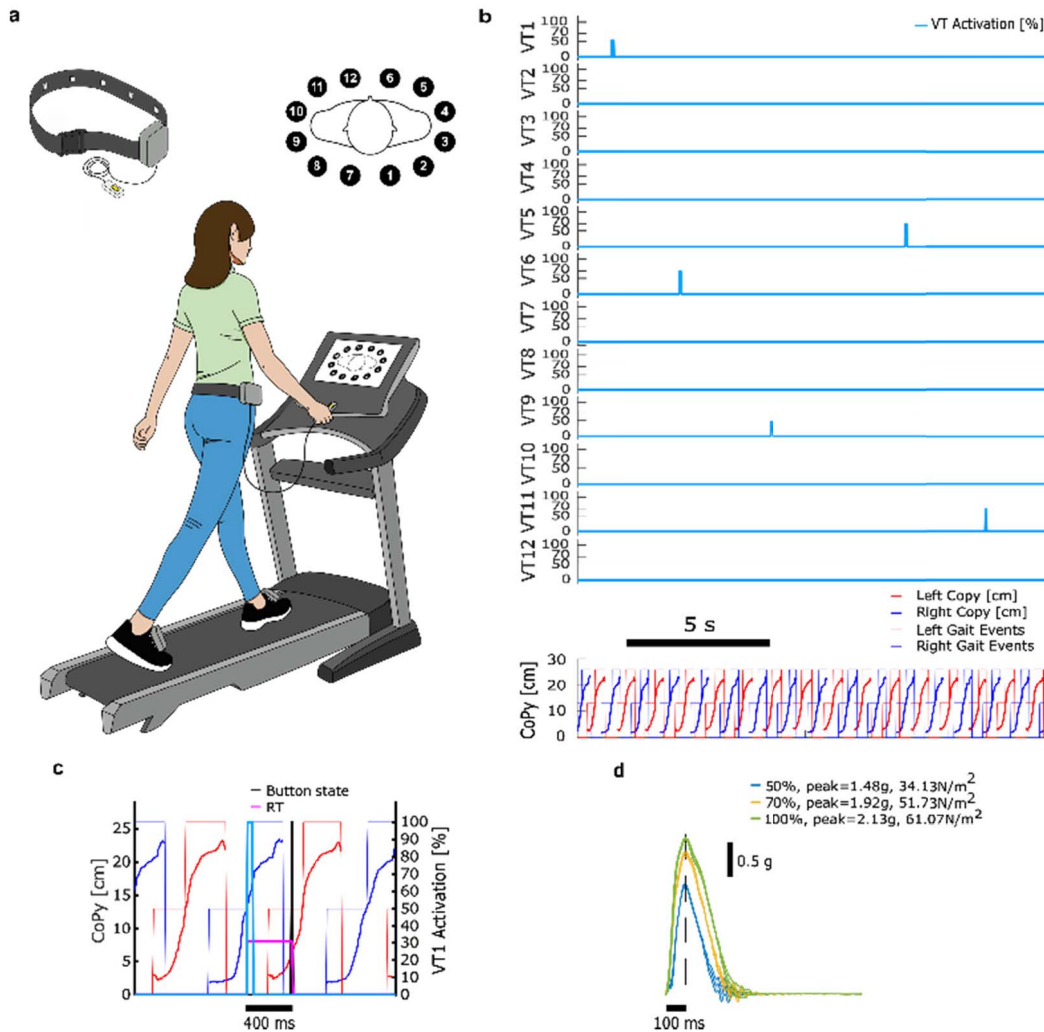


Fig. 1. Experimental set up and stimulation protocol. (a) The subject walks on a treadmill wearing the BI and holding a button for notifying the perceived vibrations. For locating the stimuli, the subject relies on a map displaying VT units configuration around the waist. (b) VT units activation sequence, with stimuli delivered on the users' waist at the occurrence of gait events. (c) Example of stimulus detection: the elapsed time between the onset of the stimulus (blue spike) and the time the subject pressed the button (black spike) corresponds to the reaction time (RT). (d) VT amplitudes corresponding to 50%, 70% and 100% duty cycles expressed in gravitational acceleration "g", when activated for 100ms in free air.

The feedback module is equipped with twelve VT units equally spaced around the waist. The belt is adjustable in size to fit users with different waist circumferences and the position of the VT units can be easily tuned manually, by means of detachable Velcro strips. In the presented experiment, the spatial distribution of the VT units was kept constant for all the participants, considering a space of 5 cm between adjacent units. Each VT unit is made of an eccentric rotating mass motor (Pico Vibe™312-101.005, Precision MicroDrives™) encapsulated in a matrix of Polydimethylsiloxane (PDMS) of 6mm thickness and 20 mm diameter, intended to increase comfort during prolonged utilization of the device, without hindering the perception of the vibrations. In fact, the larger contact area of the encapsulated VT units is expected to compensate for the damping effects of the PDMS layer on vibration propagation. Stimulation intensity is controlled with 1kHz PWM of a 5V source. Vibration amplitudes corresponding to 50%, 70% and 100% duty cycles have been characterized for 100ms activation in free air to result 1.48g, 1.92g and 2.13g peak vibration amplitudes of the VT units, respectively (Fig. 1d). Due to the coupling between amplitude

and frequency of the motors, higher vibration intensities were characterized by increased frequencies, which in this case resulted 60 Hz, 100 Hz and 150 Hz. The duration of the stimuli was set to 100 ms in consideration of the dynamics of the rotating mass motors used, to avoid overlaps between consecutive stimuli, discomfort and habituation effects [16].

B. Algorithms

Through the high-level algorithms, the mapping module executes the following operations: for each insole, it computes the single force values of the 16 sensors by (i) subtracting the output voltages recorded when no load is applied on the sensors (de-offsetting) and (ii) then applying the voltage-to-force equation identified from the preliminarily experimental characterization of the sensors described in [44]. Then, it sums the 16 force values to estimate the vertical Ground Reaction Force (vGRF) and it calculates the barycenter of the forces on the anterior-posterior direction to extract the location of the plantar Center of Pressure (CoP_{AP}). The mapping module performs the recognition of the heel-strike (HS), the

foot-flat (FF) and the toe-off (TO) as:

$$HS = k| \begin{cases} CoP_{AP}(k-1) = NaN \\ CoP_{AP}(k) < CoP_{FF} \end{cases} \quad (1)$$

$$FF = k| \begin{cases} CoP_{AP}(k-1) < CoP_{FF} \\ CoP_{AP}(k) \geq CoP_{FF} \end{cases} \quad (2)$$

$$TO = k| \begin{cases} CoP_{AP}(k-1) > CoP_{FF} \\ CoP_{AP}(k) = NaN \end{cases} \quad (3)$$

with

$$CoP_{AP}(k) = NaN \forall k | vGRF(k) < 10N \quad (4)$$

and

$$CoP_{FF} = \frac{CoP_{APmax} + CoP_{APmin}}{2} \quad (5)$$

with CoP_{APmin} and a CoP_{APmax} equal to 1.57 cm and 25.2 cm, respectively.

Synchronously with the detection of these events, specific VT units are activated to deliver time-discrete (100 ms) stimulations according to the desired feedback strategy.

C. Experimental Protocol

The feedback system was tested in a cross-sectional study involving healthy volunteers. Inclusion criteria required the subjects to be physically and mentally healthy, to have a shoe size between 41 and 43 EU and a waist circumference lower than 120 cm, for hardware limitations. Skin irritations on the stimulated area were considered as exclusion criteria. Fifteen subjects (four females; age 27 ± 2.8 ; height 174.1 ± 5.6 cm; weight 65.6 ± 8.2 kg) were recruited for the study. Prior to experiments, all the participants signed a written informed consent.

Upon arrival, participants wore the sensorized shoes and the instrumented belt. The belt was placed under the shirt, tightened to be comfortable and to secure all the VT units to be fully in contact with the skin. Before starting the experiments, a preliminary test was performed to ensure the participant could correctly perceive short vibrations of different intensities (namely $\delta_{1.48g}$, $\delta_{1.92g}$, $\delta_{2.13g}$). Specifically, the subject was instructed to stand still while the experimenter manually triggered the activation of one VT unit at one of the three pre-defined stimulation amplitudes; if the subject perceived the vibration s/he had to alert the experimenter and locate the stimulation site. All combinations of VT units and intensities were checked prior to starting the experiments, in order to ensure that the stimuli were above the user's perceptual threshold while standing. Therefore, any change of the perception observed during walking would be attributable to movement-induced attenuation [23]–[25]. A further familiarization session of about 10 minutes was performed during walking, to allow subjects to select their speed and familiarize with the VT stimuli while moving. Subjects were required to walk on the treadmill at self-selected speed without using the handrails and to focus on the perception of the stimuli. VT units were activated synchronously with the occurrence of one gait event (i.e. HS, FF, TO) at one of three stimulation

intensities, i.e. $\delta_{1.48g}$, $\delta_{1.92g}$ and $\delta_{2.13g}$. Overall, each condition (stimulation level, site and gait event) was tested 4 times, for a total of 432 stimulations (i.e. 4 repetitions, 12 sites, 3 intensities, 3 gait events). The number of repetitions of the same stimulation condition was limited to reduce trial duration. On the other hand, the number of participants was increased to promote population statistics. Even though a higher number of repetitions would have provided a more accurate assessment of the subjects' perception performance, it is reasonable to assume that the essential trends of analysis would be preserved by taking 4 repetitions for each cell of design in a cohort of 15 subjects. Considering the sagittal plane as a reference, the VT units were divided in two groups, each one associated with the gait phase of the ipsilateral lower-limb; thus, VT1-VT6 were activated with the right foot events, while activations of VT7-VT12 referred to the left ones. Subjects were given a hand-held button, which they were asked to press every time they perceived a vibration and as quickly as possible. After pressing the button, they were required to verbally state the location of the vibrating unit based on the map (Fig. 1a). Vibrations were delivered in pseudorandomized order, spaced apart from each other by a random number of strides (from 2 to 5 strides with decreasing probability, following a Poissonian distribution), to avoid expectation biases in the perception. The experiment was split in six trials to prevent from attention deficits due to prolonged trial duration. The GUI allowed the experimenter to start the trials, record the data and take note of subjects' response on the identified stimuli locations.

D. Data Analysis

Data were processed in Matlab. The following indicators were extracted from the recorded data:

- The Detection Rate (DR [%]), i.e. the percentage ratio between the number of perceived vibrations and the number of totally delivered ones.

$$DR = \frac{n_{perceived}}{n_{delivered}} \cdot 100 \quad (6)$$

- The Reaction Time (RT [ms]), i.e. the elapsed time between the onset of each stimulation and the time the subject pressed the button (Fig. 1c).

$$RT = t_{buttonpressed} - t_{VTon} \quad (7)$$

RTs were computed limitedly to the perceived vibrations.

- The Accuracy ([%]), i.e. the percentage ratio of the correctly localized stimulations over the number of totally perceived ones.

$$Accuracy = \frac{n_{correct}}{n_{perceived}} \cdot 100 \quad (8)$$

Besides Accuracy, the so-called 1-adjacent Accuracy [%], was computed, considering the identification of the unit next to the vibrating one as a correct answer. For both accuracies, missed perceptions were counted as wrong identifications.

E. Statistical Analysis

Due to the large number of missing stimulations occurring at $\delta_{1.48g}$, data of RT, Accuracy, 1-adjacent Accuracy and DR were analyzed only for two stimulation levels, namely $\delta_{1.92g}$ and $\delta_{2.13g}$. Moreover, the number of sites was reduced from twelve to six, by averaging data for each dependent variable from adjacent stimulation sites, namely VT6-VT12, VT4-VT5, VT2-VT3, VT1-VT7, VT8-VT9 and VT10-VT11. By lowering the number of levels per factor, the complexity of the statistical model is reduced to better fit the sample size. Hence, for the purpose of the statistical analysis of data, the resulting design consisted of three within-subject factors, namely the stimulation strength (*stimulation*, two levels), the stimulation site (*site*, six levels), and the events of the gait cycle to which the delivery of the stimulus was synchronized (*event*, three levels). For each cell of the design the normal distribution of the dependent variables (i.e., RT, Accuracy, 1-adjacent Accuracy and DR) was verified using the Shapiro-Wilk's test of normality. RT and Accuracy were normally distributed, whereas 1-adjacent Accuracy and DR were found highly skewed and non-normal. Accordingly, parametric tests and non-parametric tests were selected.

Parametric repeated-measures three-way ANOVAs were applied to RT and Accuracy data to investigate the existence of a statistically significant three-way interaction effect between the three within-subject factors, or any two-way interaction effect between two out of three factors. Few outliers were found in RT and Accuracy data, as assessed by inspection of multiple boxplots. However, they were not extreme, and therefore they were retained in the analysis. The sphericity assumption was tested using the Mauchly's test and the Greenhouse-Geisser correction was applied if this assumption was violated. When appropriate, post hoc pairwise comparisons were carried using the relevant correction; the partial η^2 measures were also reported. Non-parametric repeated-measures one-way ANOVAs (Friedman tests) were applied to data of 1-adjacent Accuracy and DR. If significant p -values were found, post hoc pairwise comparisons based on Wilcoxon signed-rank test were carried out using the relevant correction.

The alpha level of significance was set to 0.05 for all statistical tests. The statistical analysis was performed using IBM SPSS Statistics software package (IBM SPSS Statistics 26, SPSS IBM, New York, NY, USA).

III. RESULTS

The median values of DR at different stimulation levels are shown in Fig. 2. The DR was 50% with the lowest stimulation level, higher than 97% with $\delta_{1.92g}$, and nearly 100% with the highest level. Due to poor detection performance at the lowest stimulation strength, the measurements available for each cell of the design were roughly half of those available at the highest stimulation strengths. Therefore, the statistical analysis was restricted to $\delta_{1.92g}$ and $\delta_{2.13g}$. Results of the analysis are detailed in the following sections for each dependent variable. Data are reported as mean (M) \pm standard deviation (SD), unless otherwise stated.

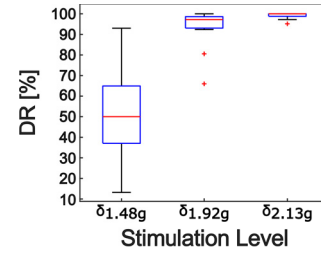


Fig. 2. Detection rate (DR) is shown for three different stimulation levels ($\delta_{1.48g}$, $\delta_{1.92g}$, and $\delta_{2.13g}$). Data are aggregated across subjects, with boxplots denoting medians and first and third quartiles.

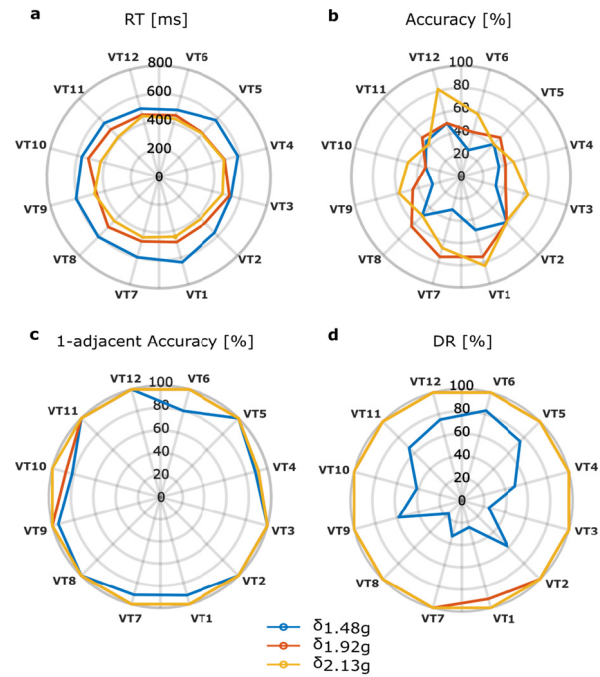


Fig. 3. Spatial distribution of (a) RT [ms], (b) Accuracy [%], (c) 1-adjacent Accuracy [%] and (d) DR [%] around the waist, at the twelve locations where VT units were placed. Data are aggregated across subjects, with values indicating medians.

A. Reaction Time

The three-way interaction effect *stimulation*site*event* was not statistically significant, $F(10,14) = 1.07$, $p = 0.39$; all two-way interaction effects were also not statistically significant: *site*event*, $F(4,29, 60.11) = 1.64$, $p = 0.17$, *stimulation*site*, $F(2,57, 35.95) = 1.74$, $p = 0.18$, and *stimulation*event*, $F(1,43, 19.97) = 1.30$, $p = 0.28$. Fig. 3a shows the spatial distribution of RT for each stimulation level, including $\delta_{1.48g}$. The increase in the stimulation strength elicited significant changes in RT ($F(1, 14) = 30.01$, $p < 0.0001$, partial $\eta^2 = 0.68$), with RT decreasing from stimulation at $\delta_{1.92g}$ (M = 509 ms, SD = 31 ms) to stimulation at $\delta_{2.13g}$ (M = 470 ms, SD = 33 ms). The main effects *site*, $F(5, 70) = 1.76$, $p = 0.13$ and *event*, $F(2, 28) = 2.14$, $p = 0.14$ were not statistically significant. Fig. 4 shows the spatial distribution of RT computed for each gait event at (a) $\delta_{1.48g}$ (b) $\delta_{1.92g}$ and (c) $\delta_{2.13g}$.

B. Accuracy

The three-way interaction effect *stimulation*site*event* was not statistically significant, $F(10, 140) = 0.99$, $p = 0.46$;

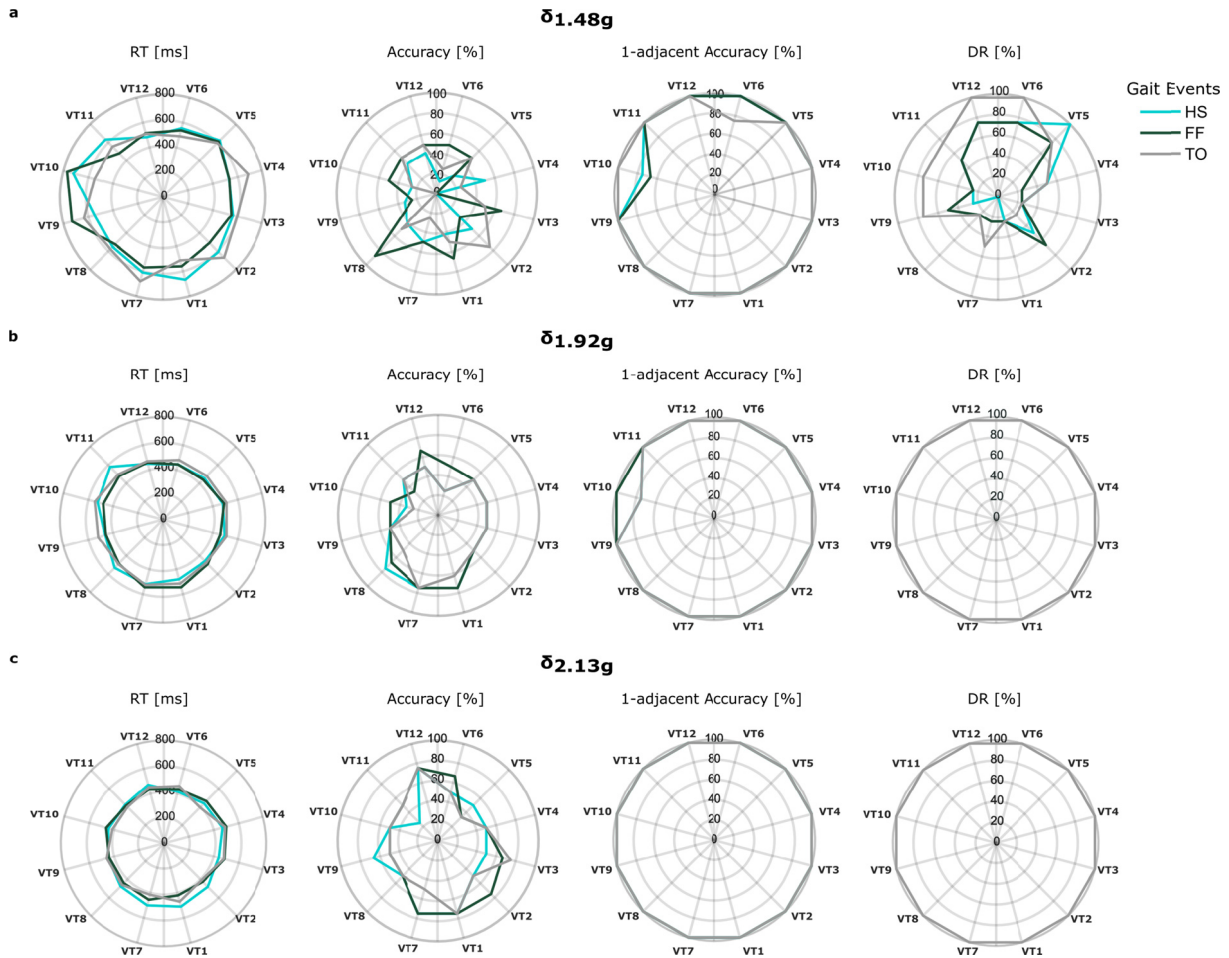


Fig. 4. Spatial distributions of RT, Accuracy, 1-adjacent Accuracy and DR calculated for each gait event (heel-strike, HS, foot-flat, FF, and toe-off, TO) at (a) $\delta_{1.48g}$ (b) $\delta_{1.92g}$ and (c) $\delta_{2.13g}$. Data are aggregated across subjects, with values indicating medians.

all two-way interaction effects were also not statistically significant: $site \times event$, $F(10, 140) = 0.54$, $p = 0.86$, $stimulation \times site$, $F(5, 70) = 2.13$, $p = 0.07$, and $stimulation \times event$, $F(2, 28) = 1.58$, $p = 0.22$. The spatial distribution of Accuracy for each stimulation level is shown in Fig. 3b, including $\delta_{1.48g}$. The main effects $stimulation$, $F(1, 14) = 14.16$, $p < 0.005$, $partial \eta^2 = 0.50$ and $site$, $F(2.69, 37.62) = 7.87$, $p < 0.001$, $partial \eta^2 = 0.36$ were statistically significant. Specifically, the increase in the stimulation strength elicited significant changes in Accuracy, which increased from stimulation at $\delta_{1.92g}$ ($M = 52\%$, $SD = 2\%$) to stimulation at $\delta_{2.13g}$ ($M = 56\%$, $SD = 2\%$). Post hoc analysis with Bonferroni adjustment revealed that Accuracy was significantly higher at sites VT1-VT7 ($M = 72\%$, $SD = 3\%$) than at VT2-VT3 ($M = 54\%$, $SD = 3\%$), VT4-VT5 ($M = 47\%$, $SD = 3\%$), VT8-VT9 ($M = 55\%$, $SD = 3\%$), and VT10-VT11 ($M = 43\%$, $SD = 3\%$), while the comparison between VT1-VT7 and VT6-VT12 ($M = 56\%$, $SD = 6\%$) was not statistically significant. Finally, the main effect $event$ was not statistically significant, $F(2, 28) = 1.11$, $p = 0.34$. Fig. 4 shows the comparison between the spatial distribution of Accuracy computed for each gait event at (a) $\delta_{1.48g}$ (b) $\delta_{1.92g}$ and (c) $\delta_{2.13g}$.

C. 1-Adjacent Accuracy

The confusion matrices associated to each stimulation level for all sites, from VT1 to VT12 are shown in Fig. 5. The

color scale provides an overview of the correct localizations and misrecognition errors, related to each VT unit. The main diagonal reflects the Accuracy, and the dispersion of colors along the sub- and super-diagonal indicates the localization mismatch with neighboring locations. While Accuracy was found depending, to some limited extent, on the specific location around the waist, the misrecognition errors turned out to be generally restricted to neighboring locations. Specifically, 1-adjacent Accuracy was introduced to accept as valid those responses that were up to one location away from the actual stimulation location. In contrast with Accuracy, 1-adjacent Accuracy turned to be highly skewed, especially at the highest stimulation level.

After averaging data across gait events, 1-adjacent Accuracy was submitted to repeated measures one-way ANOVAs (Friedman test), with $site$ as within-subject factor and $stimulation$ as moderating variable. The spatial distribution of 1-adjacent Accuracy for each stimulation level is shown in Fig. 3c. Significant differences were found across sites at $\delta_{1.92g}$, $\chi^2(5) = 13.11$, $p = 0.02$. However, pairwise comparisons performed with Bonferroni correction for multiple comparisons did not reveal any statistically significant variation of 1-adjacent Accuracy across stimulation sites. No significant differences were found across sites at $\delta_{2.13g}$. In conclusion, 1-adjacent Accuracy did not change across sites, regardless of the stimulation strength. Then, averaging across gait events

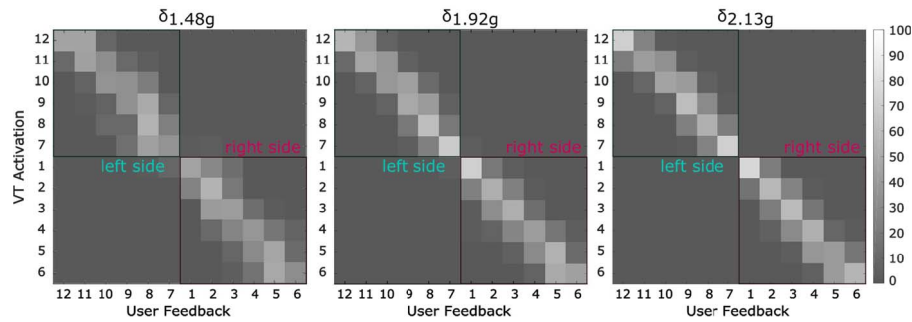


Fig. 5. The confusion matrices show the spatial spread in the stimuli localization errors.

and sites, 1-adjacent Accuracy was analyzed with *stimulation* as within-subject factor. The increase in the stimulation strength elicited a statistically significant median increase in 1-adjacent Accuracy from 96% at $\delta_{1.92g}$ to 98% at $\delta_{2.13g}$ (paired-samples Wilcoxon signed rank test: $z = 2.81$, $p = 0.005$).

Fig. 4 shows the comparison between the spatial distribution of 1-adjacent Accuracy computed for each gait event at (a) $\delta_{1.48g}$ (b) $\delta_{1.92g}$ and (c) $\delta_{2.13g}$. No statistically significant effect was found concerning the influence of gait events regardless of site and stimulation strength.

D. Detection Rate

In a similar way as for 1-adjacent Accuracy, DR was submitted to repeated measures one-way ANOVAs (Friedman test), with *site* as within-subject factor and *stimulation* as moderating variable. The spatial distribution of DR for each stimulation level is shown in Fig. 3d. No statistically significant differences emerged across sites, regardless of the stimulation strength. Then, after averaging data across gait events and sites, DR was processed considering *stimulation* as within-subject factor. The increase in the stimulation strength elicited a statistically significant median increase in DR from 97% at $\delta_{1.92g}$ to 100% at $\delta_{2.13g}$ (paired-samples Wilcoxon signed rank test: $z = 3.19$, $p = 0.001$).

Fig. 4 shows the comparison between the spatial distribution of DR computed for each gait event at (a) $\delta_{1.48g}$ (b) $\delta_{1.92g}$ and (c) $\delta_{2.13g}$. No statistically significant effect was detected concerning the influence of gait events on DR regardless of the site and the stimulation strength.

IV. DISCUSSION

Haptic displays are emerging technologies for sensory augmentation in mobility tasks, in which sight and hearing are already heavily taxed. In order to design haptic interfaces that simply and effectively convey information needed to the accomplishment of specific tasks, the study of tactile sensitivity is crucial. In particular, a deep understanding of how tactile sensitivity varies on the human body and with respect to specific movements, especially in the regions directly involved in motor activity, can provide valuable guidelines in the implementation of both hardware and software. In this respect, the waist constitutes a potentially promising stimulation site, because it is relatively stable during ambulation and therefore

little exposed to perturbations. Based on this assumption, this study investigated the perception of VT stimuli on the waist during walking.

A. Waist Perception Threshold

Firstly, human's ability to perceive time-discrete vibrations around the waist during walking was investigated, by delivering short-lasting stimuli at the occurrence of gait events. DR and RT associated to three different vibration amplitudes applied to twelve loci on the body trunk were evaluated, to examine the effect of the stimulation level on the perception. Waist perception threshold was assessed by measuring the DR for each amplitude. Results revealed that the detection performance encountered at the lowest intensity stimulus was poor compared to the other stimulation amplitudes (Fig. 2, 50% with the lowest stimulation level, higher than 97% with $\delta_{1.92g}$ level, and 100% with the highest level) and the interquartile range of the DR associated to $\delta_{1.48g}$ resulted to be larger with respect to the other levels, denoting an increased inter-subject variability in perceiving the weakest stimuli. These observations suggest that the waist perception threshold for VT stimuli in dynamic conditions falls between $\delta_{1.48g}$ and $\delta_{1.92g}$. As expected, the maximum level showed the best performance. Nevertheless, at $\delta_{1.92g}$ vibrations were already clearly perceived by the subjects. For long-term use, above-threshold stimuli such as $\delta_{1.92g}$ would be a preferable choice for providing a perceivable feedback, without the possible discomfort and skin adaptation effects introduced by higher intensity vibrations.

The RT decreased by increasing the stimulation strength (Fig. 3a), and statistically significant differences were found between $\delta_{1.92g}$ ($M = 509$ ms, $SD = 31$ ms) and $\delta_{2.13g}$ ($M = 470$ ms, $SD = 33$ ms). A similar trend was observed by Sharma *et al.* [14], who compared the RTs produced by three vibration frequencies applied on the thigh in sitting condition: 140 Hz, 180 Hz, and 220 Hz (corresponding to 1.22g, 1.58g and 1.92g, respectively), with the lowest frequency resulting in the longest RT (711 ms, 623 ms and 584 ms, respectively with 140 Hz, 180 Hz and 220 Hz). The shortest RT was obtained at 220 Hz. In the presented experiment, when a vibration of the same amplitude (1.92g) but lower frequency (100 Hz) was applied on the waist during walking, the response of participants was quicker than in [14], with RT of 509 ms against 584 ms. Here it is worth reminding that in [14] stimuli

were delivered in sitting conditions and that the RT at the thigh is likely to increase during walking due to masking effects. For this reason, the presented results strengthen the idea that the waist is a valid stimulation site candidate for locomotion assistive feedback. During static activities such as sitting or standing, relatively slow postural adjustments are needed to maintain balance. In contrast, walking is a dynamic task with a step cycle duration of about 1s for which fast motor responses are required. In this context, a RT of 470 ms can affect the decision-making process. Longest RT is attributed to the time the brain takes to process the information and plan a motor response. According to Hick's law [46], the processing time increases when multiple stimuli are presented or when there is uncertainty about the locus and the occurrence of the forthcoming stimulus. In the presented study, the stimulation site, the occurrence and the amplitude of the vibrations were randomized, generating uncertainty. In a real application, in which the subjects are exposed to predefined stimulation patterns, the RT would benefit from stimuli expectation. An aspect to consider in the design of haptic devices and that affects the RT is the overall latency of the system. In this study the wireless communication delay was 10 ms and, because of the negligible computational time to trigger motors activation, the only other source of delay was the time taken by the VT unit to reach a perceivable vibration amplitude (Fig. 1d).

B. Effect of Stimulation Sites

When analyzing the spatial distribution of DR across the stimulation sites (Fig. 3d), the detection performance was found not to be affected by the stimulation site, regardless of the stimulation strength ($\delta_{1.92g}$ or $\delta_{2.13g}$). Similarly, the RT (Fig. 3a), did not vary across the abdominal circumference when stimulating at $\delta_{1.92g}$ and at $\delta_{2.13g}$, suggesting that the RT is not affected by the site. In [14] the authors found that the RT to stimuli applied on the thigh in static conditions varied across the four locations tested, with the anterior region resulting in quicker RT than the lateral, medial and posterior regions. The invariance of the RT with the stimulation site supports the idea that the waist is a good region for providing tactile feedback, both in static and dynamic conditions.

Along with the analysis of the DR and the RT, users' ability to localize the stimuli across twelve sites on the waist was examined. The location and the spacing between stimulation sites are the main factors influencing the localization accuracy of tactile stimuli. Cholewiak *et al.* [40] analyzed the localization accuracy of VT stimuli with respect to the number of tactors and the body site on the abdomen in static conditions. When testing twelve sites, they found that the ability to localize the stimulus was a function of proximity to the spine and the navel, with higher accuracy in the case of vibrations applied to sites adjacent to these loci. By reducing the number of stimulation sites from twelve (intertactor spacing of 7.2 cm) to six (14 cm) the accuracy improved, resulting in 74%, 92% and 97% for twelve, eight and six sites, respectively. In the presented study the localization accuracy was analyzed during walking. Overall the Accuracy resulted to be lower than [40]

for all the stimulation strengths, as shown in the radar plot (Fig. 3b). As for DR and RT, the Accuracy resulted to improve with higher stimulation levels, with differences between $\delta_{1.92g}$ and $\delta_{2.13g}$.

The superiority of navel and spine with respect to the other loci in localizing the stimuli found in static conditions [3], [4], [40], [41] was also confirmed during walking. Indeed, the Accuracy resulted to be significantly higher at VT1-VT7 (spine) than at VT2-VT3, VT4-VT5, VT8-VT9 and VT10-VT11, while no differences were found between VT1-VT7 and VT6-VT12 (navel). The confusion matrices highlight that most of the misrecognition errors were restricted to neighboring locations, suggesting that the spacing between stimulation sites strongly affected the stimulus localization. In this study the vibrating units were spaced 5 cm apart, which is lower than the intertactor spacing tested by Cholewiak *et al.* (i.e. 7.2 cm), and this might have contributed to the finer identification of variable localization performance of the subjects for all the stimulation levels. The hypothesis is supported by the spatial distribution of 1-adjacent Accuracy (Fig. 3c), which reached almost 100% at $\delta_{1.92g}$ and $\delta_{2.13g}$. The increase in the stimulation strength elicited a statistically significant increase in 1-adjacent Accuracy from 96% at $\delta_{1.92g}$ to 98% at $\delta_{2.13g}$, while no variations were found across stimulation sites regardless of the stimulation strength. In summary, the analysis of the accuracies evidenced that increasing VT units spacing, and stimulus intensity can improve the localization performance. The comparison between Accuracy and 1-adjacent Accuracy, provided evidence that with an intertactor distance of 5 cm the stimulation sites are too close to be accurately identified. When the spacing is increased up to 10 cm, overall localization performance improves for all stimulation strengths and above-threshold vibrations can be successfully localized with no differences across sites.

C. Influence of Gait Events

Finally, the effect of gait events on the detection and localization of VT stimuli on the abdomen was investigated. During walking, specific gait events are characterized by different conditions, such as presence and intensity of ground reaction forces, and extension or contraction of specific muscles, which might result in a non-uniform perception throughout the gait cycle. For example, at heel-strike, high ground reaction forces might mask the haptic stimuli or decrease the localization accuracy. Especially on lower limbs, which are directly involved in the walking movements, the detection of vibrations may be significantly altered in correspondence of specific gait events. In this study, vibrations were delivered on the users' waist, synchronously with the occurrence of gait phase transitions. This stimulation strategy allowed computing the DR, RT and accuracies for each stimulation strength, site and gait event (Fig. 4). Statistically significant differences were not found in all dependent variables as function of the gait events in all the tested conditions (stimulation levels and sites).

This result indicates that the perception of VT stimuli on the abdomen is invariant with gait phase transitions. Thus, stimuli detection capability and localization accuracy are preserved on

the waist throughout the step cycle. These findings strongly impact on the design of sensory feedback interfaces and control strategies. A straightforward consequence of these findings is that when haptic stimuli are delivered on the waist, the same stimulation intensity can be used during the whole stride period, thus reducing the complexity associated to the tuning of the stimulation level in concomitance with specific gait events. Therefore, the intensity of the stimulation is now a free parameter that can be used in the design of a stimulation strategy to encode some other kind of information useful in the accomplishment of the desired task. It is worth noticing that this is the first study analyzing the effect of gait phases on tactile perception on the abdomen. When considering other body regions, most of the studies focused on how movement affects the perception, regardless of specific gait events. Notwithstanding this, as suggested by [15], [22], the perception on specific sites such as the thigh or the foot might be strongly affected by gait phases. Understanding such influence can provide useful guidelines for the design of haptic interfaces, which include the stimulation timing (i.e., whether the stimuli should be given when muscles are contracted/relaxed or during a specific phase of the gait cycle), site (i.e., stimuli applied to different regions of the skin may be subjected to different gating mechanisms) and intensity (stimuli masking effects may require the increase of the stimulation strength).

In a final remark, these findings support the idea that the waist is a promising body region for conveying information via tactile feedback during walking. Despite a decent sensitivity to stimuli detection, the perception on the waist does not degrade significantly with movements and is not affected by gait events. Such features are unique among commonly used stimulation sites and might be harnessed in the design of novel haptic feedback devices paving the way to a wide range of application scenarios, such as navigation in real and virtual environments, rehabilitation, sensory substitution and telepresence.

D. Guidelines for the Design of Wearable Haptic Interfaces for Assisting Impaired Subjects

Focusing on wearable technologies for assisting users with sensory impairments, the results of the study can be exploited in the development of VT belts for blind walkers [2], [6], in terms of stimulation parameters and number of factors to be used to effectively convey instructional cues (e.g. *stop* or *turn right/left*). In particular, the minimum distance between VT units should be set to 10 cm to allow accurate stimuli localization, an ability that is crucial when multiple units are used to deliver directional cues [3], [40], [41]. In terms of stimulation parameters, vibrations of 1.92g and 100 Hz can be successfully perceived and localized uniformly around the abdomen. A further increment of 0.21 g and 50 Hz in the stimulation strength allows to improve the perception performance, eliciting a reduction of 39 ms in the RT, and enhancements of 3% and 2% in stimuli detection and localization ability, respectively. Such stimulation parameters should be considered as a requirement in the selection of the

VT unit. In lower limb amputees and patients with neurological diseases, waist displays can be used for gait rehabilitation, ensuring the effective transmission of stimuli throughout the gait cycle, with no attenuations due to specific gait events. Spatio-temporal information can be intuitively mapped onto the torso. For example, the heel-to-toe movement of the CoP under the foot or the gait-phase transitions sequence [10] can be represented in the VT pattern, by sequentially activating the VT units from the spine to the navel. Furthermore, the possibility to stimulate both the right and the left side of the waist allows delivering bilateral stimuli, informing the patient on the status of the ipsilateral limb or conveying rhythmic cues to improve gait performance. However, it is worth reminding that the study described in this paper involved healthy young adults walking on a treadmill. Factors such as age, body-mass index, mobility level, and type and extent of the sensory impairment, as well as walking overground, might affect stimuli perception and should be considered in the selection of the optimal stimulation pattern and parameters when the system is administered to impaired subjects. Furthermore, compared to other body regions, such as hands or feet, the waist can be perceived as an unnatural location for tactile feedback. A proper training with the wearable system is strongly recommended to set the optimal vibration parameters and to guide the patients in understanding how to interpret and exploit the haptic feedback.

ACKNOWLEDGMENT

N. Vitiello and S. Crea have interests in IUVO S.r.l., a spin off company of SSSA. The technology of the sensorized insoles described in this work has been exclusively licensed to IUVO S.r.l.

REFERENCES

- [1] S. J. Lederman and R. L. Klatzky, "Haptic perception: A tutorial," *Attention, Perception Psychophys.*, vol. 71, no. 7, pp. 1439–1459, Oct. 2009, doi: [10.3758/APP.71.7.1439](https://doi.org/10.3758/APP.71.7.1439).
- [2] G. Flores, S. Kurniawan, R. Manduchi, E. Martinson, L. M. Morales, and E. A. Sisbot, "Vibrotactile guidance for wayfinding of blind walkers," *IEEE Trans. Haptics*, vol. 8, no. 3, pp. 306–317, Jul. 2015, doi: [10.1109/TOH.2015.2409980](https://doi.org/10.1109/TOH.2015.2409980).
- [3] J. B. F. V. Erp, H. A. H. C. V. Veen, C. Jansen, and T. Dobbins, "Waypoint navigation with a vibrotactile waist belt," *ACM Trans. Appl. Perception*, vol. 2, no. 2, pp. 106–117, Apr. 2005, doi: [10.1145/1060581.1060585](https://doi.org/10.1145/1060581.1060585).
- [4] J. B. Van Erp, "Presenting directions with a vibrotactile torso display," *Ergonomics*, vol. 48, no. 3, pp. 302–313, Feb. 2005, doi: [10.1080/0014013042000327670](https://doi.org/10.1080/0014013042000327670).
- [5] R. W. Lindeman, J. L. Sibert, E. Mendez-Mendez, S. Patil, and D. Phifer, "Effectiveness of directional vibrotactile cueing on a building-clearing task," in *Proc. SIGCHI Conf. Hum. Factors Comput. Syst. (CHI)*, 2005, p. 271, doi: [10.1145/1054972.1055010](https://doi.org/10.1145/1054972.1055010).
- [6] L. Wang, N. Li, D. Ni, and J. Wu, "Navigation system for the visually impaired individuals with the kinect and vibrotactile belt," in *Proc. IEEE Int. Conf. Robot. Biomimetics (ROBIO)*, Dec. 2014, pp. 1874–1879, doi: [10.1109/ROBIO.2014.7090609](https://doi.org/10.1109/ROBIO.2014.7090609).
- [7] S. Shokur *et al.*, "Assimilation of virtual legs and perception of floor texture by complete paraplegic patients receiving artificial tactile feedback," *Sci. Rep.*, vol. 6, no. 1, p. 32293, Sep. 2016, doi: [10.1038/srep32293](https://doi.org/10.1038/srep32293).
- [8] F. Sorgini *et al.*, "Neuromorphic vibrotactile stimulation of fingertips for encoding object stiffness in telepresence sensory substitution and augmentation applications," *Sensors*, vol. 18, no. 1, p. 261, Jan. 2018, doi: [10.3390/s18010261](https://doi.org/10.3390/s18010261).
- [9] R. E. Fan *et al.*, "Pilot testing of a haptic feedback rehabilitation system on a lower-limb amputee," in *Proc. ICME Int. Conf. Complex Med. Eng.*, Apr. 2009, pp. 1–4, doi: [10.1109/ICME.2009.4906637](https://doi.org/10.1109/ICME.2009.4906637).

- [10] S. Crea, B. B. Edin, K. Knaepen, R. Meeusen, and N. Vitiello, "Time-discrete vibrotactile feedback contributes to improved gait symmetry in patients with lower limb amputations: Case series," *Phys. Therapy*, vol. 97, no. 2, pp. 198–207, Feb. 2017, doi: [10.2522/ptj.20150441](https://doi.org/10.2522/ptj.20150441).
- [11] P. B. Shull and D. D. Damian, "Haptic wearables as sensory replacement, sensory augmentation and trainer—A review," *J. NeuroEng. Rehabil.*, vol. 12, no. 1, p. 59, Dec. 2015, doi: [10.1186/s12984-015-0055-z](https://doi.org/10.1186/s12984-015-0055-z).
- [12] F. Clemente, M. D'Alonzo, M. Controzzi, B. B. Edin, and C. Cipriani, "Non-invasive, temporally discrete feedback of object contact and release improves grasp control of closed-loop myoelectric transradial prostheses," *IEEE Trans. Neural Syst. Rehabil. Eng.*, vol. 24, no. 12, pp. 1314–1322, Dec. 2016, doi: [10.1109/TNSRE.2015.2500586](https://doi.org/10.1109/TNSRE.2015.2500586).
- [13] A. Sharma, M. J. Leineweber, and J. Andrysek, "Effects of cognitive load and prosthetic liner on volitional response times to vibrotactile feedback," *J. Rehabil. Res. Develop.*, vol. 53, no. 4, pp. 473–482, 2016, doi: [10.1682/JRRD.2015.04.0060](https://doi.org/10.1682/JRRD.2015.04.0060).
- [14] A. Sharma, R. Torres-Moreno, K. Zabjek, and J. Andrysek, "Toward an artificial sensory feedback system for prosthetic mobility rehabilitation: Examination of sensorimotor responses," *J. Rehabil. Res. Develop.*, vol. 51, no. 6, pp. 907–917, 2014, doi: [10.1682/jrrd.2013.07.0164](https://doi.org/10.1682/jrrd.2013.07.0164).
- [15] S. Crea, C. Cipriani, M. Donati, M. C. Carrozza, and N. Vitiello, "Providing time-discrete gait information by wearable feedback apparatus for lower-limb amputees: Usability and functional validation," *IEEE Trans. Neural Syst. Rehabil. Eng.*, vol. 23, no. 2, pp. 250–257, Mar. 2015, doi: [10.1109/TNSRE.2014.2365548](https://doi.org/10.1109/TNSRE.2014.2365548).
- [16] E. C. Wentink, A. Mulder, J. S. Rietman, and P. H. Veltink, "Vibrotactile stimulation of the upper leg: Effects of location, stimulation method and habituation," in *Proc. Annu. Int. Conf. IEEE Eng. Med. Biol. Soc.*, Aug. 2011, pp. 1668–1671, doi: [10.1109/IEMBS.2011.6090480](https://doi.org/10.1109/IEMBS.2011.6090480).
- [17] C. E. Chapman, M. C. Bushnell, D. Miron, G. H. Duncan, and J. P. Lund, "Sensory perception during movement in man," *Exp. Brain Res.*, vol. 68, no. 3, pp. 516–524, Nov. 1987, doi: [10.1007/BF00249795](https://doi.org/10.1007/BF00249795).
- [18] L. J. Post, I. C. Zompa, and C. E. Chapman, "Perception of vibrotactile stimuli during motor activity in human subjects," *Exp. Brain Res.*, vol. 100, no. 1, pp. 107–120, Jul. 1994, doi: [10.1007/BF00227283](https://doi.org/10.1007/BF00227283).
- [19] P. Paalasmaa, P. Kempainen, and A. Pertovaara, "Modulation of skin sensitivity by dynamic and isometric exercise in man," *Eur. J. Appl. Physiol. Occupational Physiol.*, vol. 62, no. 4, pp. 279–285, 1991, doi: [10.1007/BF00571553](https://doi.org/10.1007/BF00571553).
- [20] R. J. Milne, A. M. Aniss, N. E. Kay, and S. C. Gandevia, "Reduction in perceived intensity of cutaneous stimuli during movement: A quantitative study," *Exp. Brain Res.*, vol. 70, no. 3, pp. 569–576, May 1988, doi: [10.1007/BF00247604](https://doi.org/10.1007/BF00247604).
- [21] D. Hecht, M. Reiner, and A. Karni, "Enhancement of response times to bi- and tri-modal sensory stimuli during active movements," *Exp. Brain Res.*, vol. 185, no. 4, pp. 655–665, Mar. 2008, doi: [10.1007/s00221-007-1191-x](https://doi.org/10.1007/s00221-007-1191-x).
- [22] J. Duysens, A. A. M. Tax, S. Nawijn, W. Berger, T. Prokop, and E. Altenmüller, "Gating of sensation and evoked potentials following foot stimulation during human gait," *Exp. Brain Res.*, vol. 105, no. 3, pp. 423–431, Feb. 1990, doi: [10.1007/BF00233042](https://doi.org/10.1007/BF00233042).
- [23] I. Jiang and B. Hannaford, "Comparison of reaction times while walking," in *Proc. IEEE Int. Conf. Rehabil. Robot. (ICORR)*, Aug. 2015, pp. 345–349, doi: [10.1109/ICORR.2015.7281223](https://doi.org/10.1109/ICORR.2015.7281223).
- [24] I. Karuei, K. E. MacLean, Z. Foley-Fisher, R. MacKenzie, S. Koch, and M. El-Zohairy, "Detecting vibrations across the body in mobile contexts," in *Proc. Annu. Conf. Hum. Factors Comput. Syst. (CHI)*, 2011, p. 3267, doi: [10.1145/1978942.1979426](https://doi.org/10.1145/1978942.1979426).
- [25] M. A. B. Husman, H. F. Maqbool, M. I. Awad, and A. A. Dehghani-Sani, "Portable haptic device for lower limb amputee gait feedback: Assessing static and dynamic perceptibility," in *Proc. Int. Conf. Rehabil. Robot. (ICORR)*, Jul. 2017, pp. 1562–1566, doi: [10.1109/ICORR.2017.8009470](https://doi.org/10.1109/ICORR.2017.8009470).
- [26] J. C. Stevens and K. K. Choo, "Spatial acuity of the body surface over the life span," *Somatosensory Motor Res.*, vol. 13, no. 2, pp. 153–166, Jan. 1996, doi: [10.3109/08990229609051403](https://doi.org/10.3109/08990229609051403).
- [27] S. Weinstein, "Intensive and extensive aspects of tactile sensitivity as a function of body part, sex, and laterality," in *The Skin Senses*, D. R. Kenshalo, Ed. Springfield, IL, USA: Thomas, 1968, pp. 195–222.
- [28] L. A. Jones, B. Lockyer, and E. Piatieski, "Tactile display and vibrotactile pattern recognition on the torso," *Adv. Robot.*, vol. 20, no. 12, pp. 1359–1374, Jan. 2006, doi: [10.1163/156855306778960563](https://doi.org/10.1163/156855306778960563).
- [29] P. P. Kaddake, B. J. Benda, P. B. Schmidt, and C. Wall, "Vibrotactile display coding for a balance prosthesis," *IEEE Trans. Neural Syst. Rehabil. Eng.*, vol. 11, no. 4, pp. 392–399, Dec. 2003, doi: [10.1109/TNSRE.2003.819937](https://doi.org/10.1109/TNSRE.2003.819937).
- [30] A. D. Goodworth, C. Wall, and R. J. Peterka, "Influence of feedback parameters on performance of a vibrotactile balance prosthesis," *IEEE Trans. Neural Syst. Rehabil. Eng.*, vol. 17, no. 4, pp. 397–408, Aug. 2009, doi: [10.1109/TNSRE.2009.2023309](https://doi.org/10.1109/TNSRE.2009.2023309).
- [31] C. Wall and M. S. Weinberg, "Balance prostheses for postural control," *IEEE Eng. Med. Biol. Mag.*, vol. 22, no. 2, pp. 84–90, Mar. 2003, doi: [10.1109/EMEMB.2003.1195701](https://doi.org/10.1109/EMEMB.2003.1195701).
- [32] C. Lauretti *et al.*, "A vibrotactile stimulation system for improving postural control and knee joint proprioception in lower-limb amputees," in *Proc. 26th IEEE Int. Symp. Robot Hum. Interact. Commun. (RO-MAN)*, Aug. 2017, pp. 88–93, doi: [10.1109/ROMAN.2017.8172285](https://doi.org/10.1109/ROMAN.2017.8172285).
- [33] M. Filosa *et al.*, "A new sensory feedback system for lower-limb amputees: Assessment of discrete vibrotactile stimuli perception during walking," in *Wearable Robotics: Challenges and Trends* (Biosystems & Biorobotics), vol. 22. Cham, Switzerland: Springer, 2019, pp. 105–109.
- [34] I. Cesini *et al.*, "A wearable haptic feedback system for assisting lower-limb amputees in multiple locomotion tasks," in *Proc. Int. Symp. Wearable Robot.*, vol. 22, 2019, pp. 115–119.
- [35] A. Sie, D. Boe, and E. Rombokas, "Design and evaluation of a wearable haptic feedback system for lower limb prostheses during stair descent," in *Proc. 7th IEEE Int. Conf. Biomed. Robot. Biomechatronics (Biorob)*, Aug. 2018, pp. 219–224, doi: [10.1109/BIOROB.2018.8487652](https://doi.org/10.1109/BIOROB.2018.8487652).
- [36] A. Sie, J. Realmuto, and E. Rombokas, "A lower limb prosthesis haptic feedback system for stair descent," in *Proc. Design Med. Devices Conf.*, Apr. 2017, Art. no. V001T05A004, doi: [10.1115/DMD2017-3409](https://doi.org/10.1115/DMD2017-3409).
- [37] D. Zambarbieri, M. Schmid, and G. Verni, "Sensory feedback for lower limb prostheses," in *Intelligent Systems and Technologies in Rehabilitation Engineering*, Dec. 2001, pp. 129–151.
- [38] P. Marayong *et al.*, "Vibrotactile device for rehabilitative training of persons with lower-limb amputation," in *Proc. IEEE Healthcare Innov. Conf. (HIC)*, Oct. 2014, pp. 157–160, doi: [10.1109/HIC.2014.7038898](https://doi.org/10.1109/HIC.2014.7038898).
- [39] A. Plauche, D. Villarreal, and R. D. Gregg, "A haptic feedback system for phase-based sensory restoration in above-knee prosthetic leg users," *IEEE Trans. Haptics*, vol. 9, no. 3, pp. 421–426, Jul. 2016, doi: [10.1109/TOH.2016.2580507](https://doi.org/10.1109/TOH.2016.2580507).
- [40] R. W. Cholewiak, J. C. Brill, and A. Schwab, "Vibrotactile localization on the abdomen: Effects of place and space," *Perception Psychophysics*, vol. 66, no. 6, pp. 970–987, Aug. 2004, doi: [10.3758/BF03194989](https://doi.org/10.3758/BF03194989).
- [41] J. Van Erp, "Tactile displays for navigation and orientation: Perception and behavior," Utrecht Univ., Utrecht, The Netherlands, Tech. Rep., 2007.
- [42] J. B. F. Van Erp, "Tactile displays for navigation and orientation: Perception and behavior," Ph.D. dissertation, Utrecht Univ., Utrecht, The Netherlands, 2007.
- [43] M. Donati *et al.*, "A flexible sensor technology for the distributed measurement of interaction pressure," *Sensors*, vol. 13, no. 1, pp. 1021–1045, Jan. 2013, doi: [10.3390/s130101021](https://doi.org/10.3390/s130101021).
- [44] S. Crea, M. Donati, S. De Rossi, C. Oddo, and N. Vitiello, "A wireless flexible sensorized insole for gait analysis," *Sensors*, vol. 14, no. 1, pp. 1073–1093, Jan. 2014, doi: [10.3390/s140101073](https://doi.org/10.3390/s140101073).
- [45] D.-S. Kim and H. Tran-Dang, "An overview of ultra-wideband technology and its applications," in *Industrial Sensors and Controls in Communication Networks*. Cham, Switzerland: Springer, 2019, pp. 181–196.
- [46] L. E. Longstreth, N. El-Zahhar, and M. B. Alcorn, "Exceptions to Hick's law: Explorations with a response duration measure," *J. Exp. Psychol., Gen.*, vol. 114, no. 4, pp. 417–434, 1985, doi: [10.1037/0096-3445.114.4.417](https://doi.org/10.1037/0096-3445.114.4.417).